nature communications

Article

https://doi.org/10.1038/s41467-024-55690-0

An essential role for TASL in mouse autoimmune pathogenesis and Toll-like receptor signaling

Received: 30 July 2020

Accepted: 21 December 2024

Published online: 24 January 2025

Check for updates

Laura Lau[1,2], Taryn A. Cariaga[1,2], Abraham B. Chang[1,3], Joan H. Lane[1], Whitney E. Purtha[1], Aaron S. Rapaport[1], Ruozhen Hu[1,4], Hiroyasu Konno[1], Daryl N. Bulloch[1], Matthew J. Rardin[1], Bradford W. Gibson[1], Jason Devoss[1], Wenjun Ouyang[1,2] & Paolo S. Manzanillo[1,2]

TASL is an immune adaptor that binds to the solute carrier SLC15A4 and facilitates activation of the transcription factor IRF5 during Toll-like receptor (TLR) signaling. Similar to *IRF5* and *SLC15A4*, single nucleotide polymorphisms (SNPs) within *TASL* have been implicated in increased susceptibility to systemic lupus erythematosus (SLE) in patients. However, the biological function of *TASL* in vivo and how SLE-associated SNPs increase disease risk is unknown. Here we report that mice deficient in *Tasl* lack responses to TLR7/9 stimulation and are protected from autoimmune symptoms induced by Aldara or pristane. Loss of *Tasl* reduces IRF5 phosphorylation and cytokine production in multiple immune cell types but has no effect on other aspects of TLR signaling. Conversely, an SLE-associated *TASL* risk variant increases TASL protein expression via codon usage, resulting in augmented cytokine production in human cells. Altogether, our study validates the essential function of TASL in TLR signaling and autoimmune pathogenesis.

Systemic lupus erythematosus (SLE) is a chronic inflammatory autoimmune disease where up to 90% of all patients are women[1]. Although the exact etiology of lupus is unknown, type I interferon cytokines produced by plasmacytoid dendritic cells (pDCs) and the induction of autoantibodies by B cells are thought to play key roles in SLE pathogenesis[2,3]. Blood from humans with active SLE contain unique transcriptional signatures indicative of type I interferon (IFN) signaling[4], while depletion of pDCs or deletion of genes required for type I IFN signaling in mice results in protection from pre-clinical models of SLE[5,6]. Sensing of nucleic acids by Toll-like receptors (TLR) 7 and 9 are believed to be triggers for induction of interferons and immune activation during SLE progression[7,8]. Increased expression or auto-activation of TLRs in pre-clinical mouse models is sufficient to induce lupus like symptoms in mice[9,10].

Additionally, genome-wide association studies (GWAS) demonstrate a strong genetic component associated with development of SLE, with enrichment in genes responsible for innate immune activation, B cell development, and TLR signaling [11,12]. But despite the identification of dozens of novel genes associated with SLE, the function of these genes and how they may contribute to SLE susceptibility is poorly understood. One such gene is *TASL* in which single nucleotide polymorphisms (SNPs) were previously identified to associate with increased risk to SLE development[11]. Though TASL lacks sequence or structural homology to known proteins, studies using THP-1 and CALU-3 cell lines have elegantly demonstrated a molecular function for TASL as an SLC15A4 associated adaptor protein required for IRF5 activation upon TLR stimulation[13]. However, the role of TASL in vivo and its biological and genetic relation to lupus pathogenesis remains unexplored.

[1]Amgen Research, Amgen Inc., 720 Gateway Blvd, South San Francisco, CA 94080, USA. [2]Present address: Gilead Inc, 333 Lakeside Dr, Foster City, CA 94404, USA. [3]Present address: Exelixis Inc, 1851 Harbor Bay Pkwy, Alameda, CA 94502, USA. [4]Present address: Genentech Inc, 1 DNA Way, South San Francsico, CA 94080, USA. e-mail: Paolo.manzanillo@gmail.com

Using *Tasl* deficient mice and human cells derived from genetic carriers, we provide insight into the biological function of TASL and SLE development. We demonstrate that TASL is necessary for the cellular responses to TLR7/9 ligands both in vivo and within SLE relevant immune cells such as pDCs and B cells. Loss of TASL inhibits cellular activation of IRF5 and renders mice resistant to two chemical induced models of SLE. Additionally, a SNP associated with SLE risk can modulate TASL expression and affect TLR responses in human cells. Thus, TASL plays an obligate role in TLR7/9, SLE pathogenesis, and provides credence to the development of SLE therapeutics that disrupt the SLC15A4-TASL-IRF5 signaling pathway.

Results

TASL is essential for TLR7/9 induced cytokine production

Expression analysis of human and mice suggests that *TASL* is expressed preferentially in immune rich tissues (Supplementary Fig. 1a, b). RT-qPCR analysis of magnetically sorted immune cell populations from mouse spleens showed highest expression of *Tasl* in pDCs, followed by B cells and monocytes/myeloid cells (Supplementary Fig. 1c) suggesting a function within these cell types. To understand the biological function of TASL in vivo and within specific immune cell sub types, we generated BALB/c mice deficient in the mouse homolog of *Tasl*, hereafter referred to as $Tasl^{-/-}$ (Supplementary Fig. 1d–f). Knockout mice were normal, born at normal mendelian ratios, with no obvert pathology or decreased in life span (data not shown). Additionally, $Tasl^{-/-}$ mice displayed no homeostatic differences in immune cell subsets within B cells, T cells, and myeloid cells compared to wild type litter control mates (Supplementary Fig. 2). However, upon in vivo injection of TLR7 and TLR9 agonists, $Tasl^{-/-}$ failed to produce type I interferons (Fig. 1a) In contrast, no differences were seen between knockout mice and wild type littermate controls upon injection with the TLR4 agonist LPS, suggesting a specific role for TASL in TLR7/9 signaling in vivo.

Next, we sought to determine whether TASL plays a cell autonomous role in TLR7/9 signaling within immune cells. We isolated tissue and various immune cells from wild type and knockout mice to assess cytokine production upon stimulation. Both total splenocytes and total marrow cells from $Tasl^{-/-}$ failed to produce either IFN-β or IL-6 upon TLR7/9 stimulation but responded normally to TLR4 stimulation (Supplementary Fig. 3a, b). Identical results were observed from analysis of specific cell types derived from the spleen. Loss of TASL in splenic pDCs, B cells, and neutrophils isolated resulted in a lack of IFN-β or IL-6 secretion upon TLR7/9 stimulation (Fig. 1b). This was in contrast to bone-marrow derived macrophages and dendritic cells which displayed little to modest differences up TLR stimulation (Supplementary Fig. 3c). Stimulation of Flt3L derived pDCs with agonists for other innate immune receptors such as TLR3(poly I:C), TLR4(LPS), cGAS(ISD) and RIG-I(5'pdsRNA), showed no defects in IL-6 cytokine production between wild type and *Tasl* deficient cells (Fig. 1c). Furthermore, RT-qPCR analysis further confirmed defects not only at the cytokine production level but also on the transcription of TLR7/9 induced genes (Fig. 1d). Thus, TASL appears to play an important cell intrinsic role for production of both type I interferons and inflammatory cytokines within TLR7/9 stimulated immune cells.

TASL is required for IRF5 activation but not TLR7/9 processing

Next we sought to determine if TASL may be affecting TLR7/9 signaling directly on TLRs or by affecting proximal signaling components such as kinases and transcription factors that are activated upon TLR stimulation. Cells deficient in *Tasl* upregulated interferon responsive gene transcripts and phospho-STAT1 levels upon type I interferon treatment, suggesting that lack of IFN or cytokine production by TLR stimulation cannot be attributed to defects in IFN autocrine signaling (Supplementary Fig. 4a, b). No differences in lysosomal acidification nor TLR9 ligand uptake could be detected between wildtype and *Tasl* deficient pDCs (Supplementary Fig. 4c, data not shown). Additionally, loss of TASL did not affect TLR7 or TLR9 RNA expression in cells (Supplementary Fig. 4d). Defects in TLR7/9 processing have been shown to result in defective cell surface and intracellular expression of TLR protein[14–16]. Using antibodies that have been successfully used to detect endogenous levels of mouse TLRs[14,16,17], we found no differences in either intracellular or surface expression on TLR7/9 in pDCs derived from wildtype and $Tasl^{-/-}$ mice (Fig. 2a, data not shown). Western blot analysis of immunoprecipitation experiments using anti-TLR7 or anti-TL9 antibodies in pDCs detected no differences in TLR processing (Fig. 2b, Supplementary Fig. 4e). Additionally, loss of TASL resulted in no defects in TLR induced activation of map kinase signaling (Fig. 2c, d, Supplementary Fig. 4f, g). TLR induced phosphorylation of IκBα and STAT1 were also unaffected by TASL (Supplementary Fig. 4h). Thus, TASL does not appear to play a direct role in TLR7/9 expression, processing, or proximal kinase signaling activation, suggesting other mechanisms responsible for the defective TLR cytokine responses in *Tasl* deficient mice.

In addition to activation of map kinases and NFκB signaling pathways, TLR activation is known to mediate phosphorylation of the IRF family of transcription factors that induce production of type I interferon and pro-inflammatory cytokines[18]. TLR mediated phosphorylation of IRFs induces dimerization, binding of co-factors, and translocation to the nucleus[18,19]. Mice deficient in *Irf3*, *Irf5*, and *Irf7* have been shown to have cell type dependent defects in response to specific TLR ligands[18,19]. TASL is essential for specific activation of the transcription factor IRF5 in TLR7/9 stimulated Calu-1 and THP-1 cells lines[13] without any effect on IRF3 and IRF7 signaling. TASL serves as an IRF5 adaptor protein to mediate its activation upon TLR7/9 activation, analogous to how adaptor proteins TRIF and STING mediate IRF3 signaling[18]. To determine if $Tasl^{-/-}$ mice suffer from defects in TLR7/9 mediated activation of IRF5, we performed western blot analysis of primary pDCs and B cells derived from knockout mice upon TLR7/9 stimulation. We first validated antibodies that detected mouse IRF5 and phosphorylated IRF5 upon co-expression with its activating kinase, IKKβ (Supplementary Fig. 5a). In pDCs and B cells isolated from wild type control littermates, *Tasl* deficient cells had significantly reduced phospho-IRF5 activation kinetics upon either TLR9 stimulation (CpG A) or TLR7 stimulation (R848,R837) (Fig. 2e, f, Supplementary Fig. 5b, c). In contrast, cell types such as BMDMs that do not depend on TASL for cytokine production upon TLR7/9 stimulation, showed no defects in pIRF5 activation kinetics (Supplementary Fig. 5d). Fractionation of nuclear and cytosolic extracts from CpG A stimulated pDCs showed defects in both total and nuclear p-IRF5 (Supplementary Fig. 5e) in KO cells, consistent with IRF5 phosphorylation being required for IRF5 dimerization and nuclear translocation[13]. Although we failed to analyze endogenous IRF7, loss of TASL did not affect nuclear translocation of CopGFP-IRF7 protein upon CpG A stimulation of mRNA transfected pDC cells (Supplementary Fig. 5f). Lastly, we looked at cytokine production in other IRF5 dependent signaling pathways, such as NOD1 and NOD2 activation[20], and found defects in cytokine production in *Tasl* deficient pDCs (Supplementary Fig. 5g). Thus, TASL appears to play an essential and specific role in TLR7/9 activation of IRF5 in pDCs, B cells, and signaling pathways that require IRF5 for cytokine production.

$Tasl^{-/-}$ mice are resistant to SLE development

Next, we determined the role of TASL in SLE development in vivo using two different chemically induced mouse models of lupus. Repeated epicutaneous application of imiquimod cream (Aldara) induces systemic autoimmune disease and SLE like symptoms in BALB/c mice[21]. Treatment of wild type littermate mice with imiquimod for 8 weeks, resulted in splenomegaly and the development of anti-dsDNA antibodies (Fig. 3a–c). Additionally, treated mice had increased levels of leukocyte cells and protein within urine and acquired

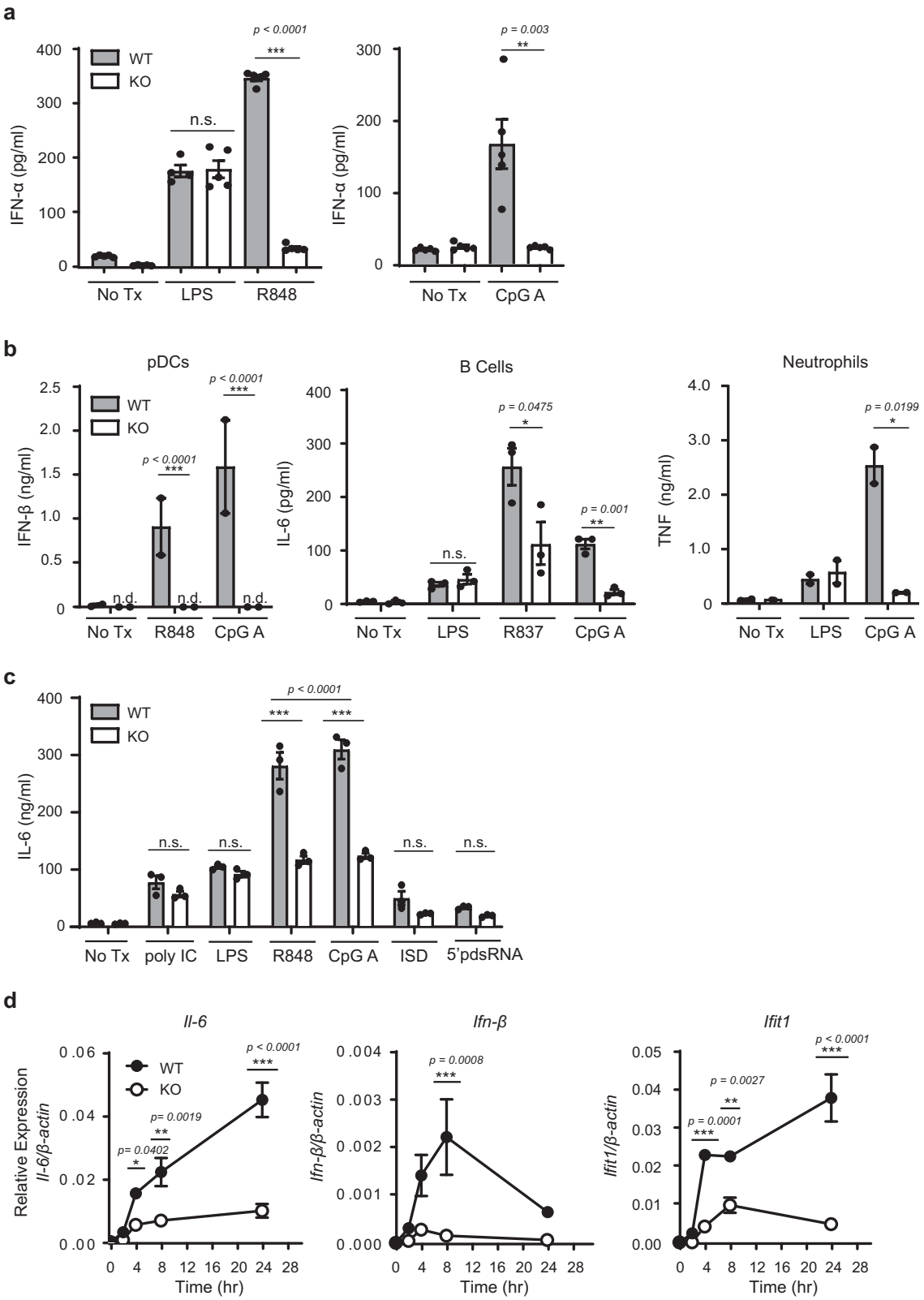

glomerulonephritis pathologies (Fig. 3d, e, Supplementary Fig. 6). In stark contrast, *Tasl*$^{-/-}$ mice displayed no such phenotypes or SLE like symptoms following imiquimod treatment and were nearly indistinguishable from PBS treated control mice (Fig. 3a–e, Supplementary Fig. 6). Similar results were also obtained using the pristane (2,6,10,14 tetramethylpentadecane TMPD) induced model of SLE, which induces the production of autoantibodies in treated mice[22]. Wild type control mice intraperitoneally injected with pristane developed autoantibodies against ribonuclear proteins (RNPs), nucleic acids (dsDNA), and nuclear antigens (sm) (Fig. 3f). In comparison, *Tasl*$^{-/-}$ mice did not develop an increase in autoantibody production following pristane injection and was indistinguishable from PBS treated control mice (Fig. 3f). Thus, genetic loss of *T*asl provides protection in mouse models of SLE and suggests an essential role for TASL in SLE disease initiation.

Fig. 1 | *Tasl*$^{-/-}$ mice show defective response to toll-like receptor 9 and 7 agonists. a Serum IFN-α levels from *Tasl*$^{-/-}$ (KO) and wild type (WT) littermate mice injected with either LPS (10 mg/kg), R848 (10 μg), or CpG A (100 μg). $n = 5$ mice for all treatment groups except WT mice treated with LPS ($n = 4$). **b** Splenic plasmacytoid dendritic cells (pDCs), B cells, and neutrophils were isolated from *Tasl*$^{-/-}$ (KO) and wild type (WT) littermate mice and stimulated with either LPS, R848, or CpG A. Cytokines were measured from supernatants either 24 h post stimulation (pDCs, neutrophils) or 48 h post stimulation (B cells). **c** Bone marrow derived Flt3L pDCs were stimulated with either poly I:C (50μg/ml), LPS (5 μg/ml), R848 (10 μg/ml), CpG A (10μg/ml), interferon stimulatory DNA ISD (4 μg/ml), or 5'pdsRNA(2 μg/ml) and IL-6 levels was measured from supernatants 24 h post stimulation. **d** RT-qPCR analysis of Type I IFN genes of WT and KO Flt3L pDCs stimulated with CpG A (1 μg/ml) for the indicated times. All data are means ± SEM and are representative of at least 2 independent experiments. Cells were isolated from 5 mice per genotype that were pooled. In (**a**), (**b**), Unpaired *t* test (2-tailed) *** $P < 0.001$, ** $P < 0.005$ In (**c**) and (**d**), Two-way ANOVA *** $P < 0.0001$; ** $P < 0.005$, * $P < 0.05$.

Characterization of a *TASL* SNP associated with SLE

Lastly, we sought to functionally characterize an SLE associated SNP within *TASL* and its relation to TLR signaling. Given our characterization of *Tasl* deficient mice, we theorized that SNPs increasing TASL expression may lead to SLE risk development due to heighted TLR responses. Previous GWAS studies identified an association between the SNP (rs887369-C) and SLE development[11]. This SNP is a synonymous variant within the Val209 (UniProt: Q9HAI6) codon position of TASL (Fig. 4a). Although carriers with the C allele have increased risk for SLE development relative to carriers with the A allele, whether rs887369 genotype affects TASL expression and function is not well known.

Since rs887369 does not alter TASL's amino acid sequence and has not been reported as an eQTL, we hypothesized that the rs887369 genotype might affect protein expression due to a change in codon usage (Fig. 4a). Changes in codon usage and the availability of charging tRNAs have been shown to have profound effects on protein translation[23,24]. Carriers with A allele result in the GUU codon, which has a usage frequency of 11%[25] (Fig. 4a). In contrast, carriers with the SLE risk C allele result in the GUG codon for Val, which has a much higher codon usage frequency of 28.1%. To test our hypothesis that the rs887369 allele could affect TASL protein translation, we first expressed TASL epitope tagged constructs in HEK293T cells encoding either the C or the A allele and analyzed RNA and protein expression. No difference in TASL mRNA expression was detected between transfected samples, suggesting that rs887369 does not affect mRNA stability or expression (Fig. 4b). In contrast, western blot analysis of transfected cells showed a consistent ~2.4 fold increase in TASL protein levels in cells expressing the C-allele risk variant versus the A-allele (Fig. 4c). This was further confirmed via in vitro translation experiments using HELA cell ribosomal extracts, in which the C-allele risk variant translated more TASL protein than the A allele carriers (Fig. 4d). Overall, this demonstrates that the rs887369 genotype may affect TASL expression at the protein level and that the rs887369-C SLE risk variant may lead to increased TASL expression.

Due to the role of TLRs and B cells in SLE progression, we next assessed the effect of TASL expression and rs887369 on TLR stimulated B cells. We first identified that CRISPR mediated deletion of *TASL* in either primary human B cells or Epstein bar immortalized B cells (BLCLs) resulted in diminished cytokine production in response to TLR stimulation (Fig. 4e, f). Conversely, mRNA transfection of TASL in primary human B cells increased responses to TLR signaling relative to control CopGFP transfection, further implicating a role of TASL expression in TLR signaling (Fig. 4g, Supplementary Fig. 7a, b). Next, we obtained rs887369 genotyped BLCLs generated from the HapMap project[26], that were homozygous at rs887369 for either the A allele, or the SLE risk C allele. Comparison between rs887369 allele carriers showed that BLCLs containing the SLE risk variant (C allele), produced higher levels of IL-6 upon TLR7 stimulation, relative to A allele carriers (Fig. 4h). All together, these data suggest that TASL can influence TLR signaling in human cells and that SNPs affecting TASL expression may increase SLE risk due to increased TLR responsiveness.

Discussion

Here we demonstrate a novel role for TASL in TLR7 and TLR9 signaling within a variety of immune cells in vitro and in vivo. TASL was found to be expressed and functional in both pDCs and B cells, two cell types that are known to contribute to lupus pathogeneis[2,3]. pDCs are believed to be the source of type I interferon signature classically associated with SLE, endowed with the ability to produce large amounts of type I interferons upon TLR7/9 engagement[5,6,27]. Conversely, B cells are thought to be activated by type I IFN cytokines produced by pDCs and by direct sensing of TLR7 and TLR9 ligands[28]. Previous single cell RNAseq experiments on patients with lupus nephritis identified high expression of TASL in pDCs and B cells clusters in diseased patients[29]. Our findings suggest that TASL may endow these cell types to respond accordingly to TLR7/9 ligands, serving as the source for type I interferons and antibodies driving disease in these patients.

In support of this, we have identified a biological basis for increased SLE development associated with TASL and the rs887369 risk variant. Mice deficient in *Tasl* did not produce type I interferons in response to TLR7/9 stimulation and developed no autoantibodies or pathology under pre-clinical models of SLE. Whereas human cells carrying an SLE risk variant that increases TASL expression had elevated cytokine responses upon TLR stimulation. Thus, levels of TASL expression may dictate the response of cells to TLR7/9 ligands and serve as a direct therapeutic target for the treatment of lupus.

Polymorphisms within *IRF5* are one of the most reproduced genetic risk factors found in GWAS studies on SLE development[11,12]. Although IRF5 was initially identified to be required for the induction of TLR7/9 signaling[19], studies on its in vivo role in SLE pathogenesis had been stymied due to the presence of a carrier mutation in the *Dock2* gene found in *Irf5* deficient mouse colonies[30–32], confounding the interpretation of past IRF5 studies. Our results provide further credence to an essential role for IRF5 signaling in SLE development. Cells from *Tasl* knockout mice have reduced IRF5 signaling upon TLR7/9 stimulation suggesting that a lack of IRF5 activation may be the underlying mechanism conferring in vivo resistance to SLE models and TLR7/9 stimulation. Our study is in agreement with findings showing TASL to be a necessary component mediating IRF5 activation in cell lines[13]. Mechanistically, TASL interacts with the solute carrier SLC15A4 and functions as an adaptor for IRF5 to facilitate IRF5 phosphorylation[13]. Interestingly, human polymorphisms in *SLC15A4* have also been associated with increased susceptibility to SLE[11,12]. And similar to *Tasl* deficient mice, *SLC15A4* knockout mice fail to respond specifically to TLR7/9 agonists in vivo[33]. Thus, we speculate that genetic risk variants in *TASL*, *SLC15A4*, and other TLR signaling components (*IRAK1*, *TLR7*)[11] maybe epistatic to *IRF5* in their contribution to SLE development.

Lastly, it is of interest to note that *TASL* is an X-chromosome gene that has previously been shown to escape X-chromosome inactivation in spleen tissue in mice and humans[34,35]. PBMCs derived from females have been shown to produce higher levels of cytokines upon TLR stimulation[36]. And female mice have been known to be more susceptible to models of autoimmunity, independent of hormone levels[37]. Several genes important for immune cell function and development reside within the X-chromosome such as *TLR7*, *FOXP3*, and *CD40LG*. Given the gender bias of SLE development in females and increased SLE susceptibility in males with Klinefelter syndrome (47,XXY)[38], we

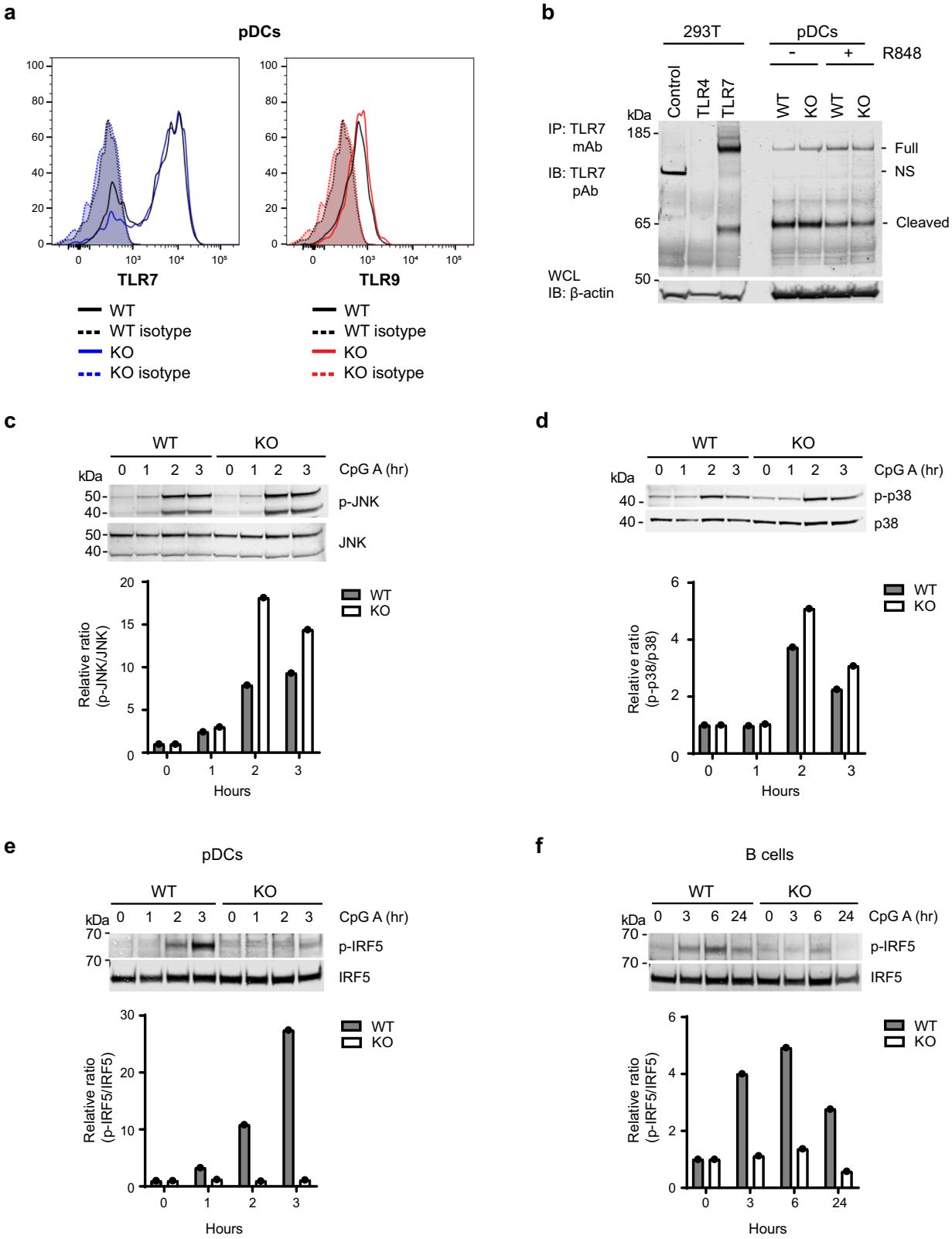

speculate that *TASL* maybe an additional factor contributing to the effects of X chromosome dosage on autoimmune disease risk.

Methods

TASL genetic information

Human *TASL* (Gene ID: 80231, UniProt: Q9HAI6; Chromosome X p21.2). SNP rs887369. Mouse *Tasl*(Gene ID: 71398).

Generation and use of *Tasl* deficient mice

Tasl$^{-/-}$ mice were generated via CRISPR in the BalbC/j substrain by Biocytogen Inc based on NCBI GeneID 71398 and transcript NM_001163539 of the mouse homolog of *Tasl*. Single guide RNA (sgRNAs) were designed to target *Tasl* DNA coding regions within intron 1 (sgRNA1: 5′-AAAATTATAAGAAGACGCTG-3′) and within the 3′UTR (sgRNA2: 5′-AAGGCCTACCATTCCAGTGC-3′). Zygotes were

Fig. 2 | *Tasl*$^{-/-}$ mice show defects in IRF5 activation. a FACS histogram overlays of TLR7 or TLR9 expression from WT and *Tasl*$^{-/-}$ (KO) mice splenic pDCs. Solid lines indicate staining with primary antibodies, while dotted lines indicate antibody isotype staining controls. **b** Immunoprecipitation (IP) of TLR7 was performed on Flt3L pDCs derived from WT or *Tasl*$^{-/-}$ (KO) mice. Western blot analysis was performed for detection of TLR7 processing. HEK293T cells stably expressing mouse TLR7 and TLR4 was used respectively as a positive and negative control. β-actin in whole cell lysate (WCL) was detected as loading control. NS indicates a non-specific band. Data are representative of at least 3 independent experiments **c** Flt3L pDCs were stimulated with CpG A (3 μM) for the indicated time points. Western blot analysis and quantification was performed for JNK and total JNK and (**d**) p38 and p-p38. **e** Western blot analysis and quantification of IRF5 and p-IRF5 in CpG A (3 μM) stimulated Flt3L pDCs at the indicated time points. **f** Western blot analysis and quantification of p-IRF5 and IRF5 in in CpG A (3μM) stimulated splenic B cells at the indicated time points. Quantification of western blot is represented as the ratio of intensities relative to time zero. $n = 5$ mice per genotype were used and pooled per experiment.

micro injected with sgRNAs complexed with CAS9, transferred to Balb/c females and founders were established and knockout mice were confirmed by polymerase chain reaction (PCR) product sequencing and were born at normal Mendelian ratios. Genotyping was confirmed by analyzing allelic presence of *Tasl* exon2 via PCR using the following DNA primers: Forward primer 5′AGCAATGTCTCCACTCCCGGC-3′, WT reverse primer 5′- GACCTACTTGGTTCCACCTTC -3′, and KO reverse primer 5′GCACTGCAGAAATCTGAAATGGC-3′.

Permission for use of animals for studies was granted by the Amgen Institutional Animal Care and Use Committee under Protocol 2009-00004. Animals were housed in a specific pathogen-free facility at Amgen under the animal housing guidelines of the Amgen Comparative Animal Research (CAR) department in an 12 h light/12 hr dark lighting cycle at 22 degree Celsius. Wild-type control (*Tasl*$^{+/+}$) and *Tasl*$^{-/-}$ mice were co-housed together. Mice were humanely euthanized by inhalation of carbon dioxide for tissue harvests and study endpoints.

Tissue and cell isolation

The following tissue samples were harvest from 6 to 8 week old female wildtype *Tasl* littermate controls: bone marrow, brain, heart, kidney, liver, lung, and spleen into Trizol (Invitrogen; 15596-018). Total RNA was harvested with RNAeasy kit (Qiagen; 74104) and treated with RNase-Free DNase set (Qiagen; 79256). Spleens were harvested from 5 to 8 week old wildtype *Tasl* littermate controls, homogenized in Miltenyi Biotec C tubes and treated with ACK lysis buffer for removal of erythrocytes. The following cells types were isolated with microbead isolation kits (Miltenyi Biotec): B cells (130-090-862), pan T cells (130-095-130), neutrophils (CD11b; 130-097-658), conventional dendritic cells (CD11c; 130-108-338), and pDCs (130-107-093). Enrichment of cell populations were confirmed by FACs analysis. Human tissue RNA samples were from the Human MTC panel I, II and Human immune system MTC panel (Takara Bio; 636742, 636743, and 636748).

TLR stimulation of mice

Various toll-like Receptor ligands such as R848 (Vaccigrade; vac-r848), CpG A (ODN1585, Vaccigrade; vac-1585-1) and Lipopolysaccharide (LPS; tlrl-b5lps) were purchased from Invivogen. Each TLR ligand was reconstituted in endotoxin free water and diluted in PBS to desired concentration. CpG A (ODN 1585) underwent an additional room temperature incubation with the liposomal transfection agent, DOTAP (Sigma Aldrich; 11202375001), ending in desired concentration of ligand. Using a 29 g insulin syringe 6–8 week old *TASL*$^{-/-}$ (KO) and wild type (WT) littermate mice received an intravenous 200 μL injection of the desired dose of ligand. At desired post stimulation timepoints (LPS 2 h, R848 4 h,CpG A 5 h), animals were subjected to 3% isoflurane and bled via their retro-orbital sinus or via a terminal cardiac puncture. Serum was used to assess cytokine and Type I IFN levels over the course of TLR stimulation.

Aldara (Imiquimod) induced systemic lupus erythematosus

Tasl$^{-/-}$ (KO) and wild type (WT) littermate mice, 6–10 week females received three times weekly application of Aldara (Imiquimod 5% cream, NDC 45802-0368-02, Perrigo) as for 8 weeks[21]. Aldara was prepared in such a manner as to allow application of 3.125 mg of cream to each animal's right ear while under manual restraint and using a cotton applicator. Animals were monitored daily by staff for adverse events common with Aldara application. The day prior to euthanasia, each animal's urine was collected into sterile petri dishes and urinalysis for protein, blood and leukocytes was measured using proteinuria strips (Fisherbrand; 23-111-262). At 8 weeks, animals were sacrificed via 3.5% isoflurane, cardiac puncture and cervical dislocation. Blood was used for serum autoantibody production analysis, kidneys were collected for either histopathology (10% neutral buffered formalin, NBF), RNA analysis or flow cytometry (RPMI media).

Pristane induced systemic lupus erythematosus

Prior to immunization, all *Tasl*$^{-/-}$ (KO) and wild type (WT) littermate mice, 6–10 week females animals were bled via retro orbital sinus for baseline serum autoantibody production. Sterile-filtered, endotoxin tested Pristane at >95% purity was purchased from Sigma Aldrich (P9622). Animals were manually restrained and, using a 27 g glass syringe, were intraperitoneally injected with 200uL of solution. Animals were monitored daily by staff and were bled via retro orbital sinus every other month for serum analysis. After 8 months post pristane immunization, animals were euthanized, and serum was collected via cardiac puncture.

Kidney histology analysis

Left kidneys from female wild type (WT) and *Tasl*$^{-/-}$ (KO) littermate mice treated with IMQ were collected and preserved in 10% NBF, transferred to 70% ETOH, paraffin embedded, sectioned and stained with hematoxylin and eosin (H&E) or Periodic Acid Schiff (PAS). Glass slides were examined by light microscopy. Specimens were evaluated by a veterinary pathologist and scored according to pre-established criteria outlined for glomerular lesion classifications[21,39]. Four lesion categories: mesangioproliferation, endocapillary hypercellularity, mesangial matrix expansion, and segmental sclerosis were individually graded on a semiquantive scale of 0–2 based on the percent of affected glomeruli (0 = < 10%, 1 = 10–50%, 2 > 50%). A summed composite score for the four lesion categories was calculated for each animal (Range 0–8; Fig. 3e).

Cell lines, and tissue culture

HEK293 T cells were purchased from American Type Culture Collection (ATCC; CRL-3216) and cultured in DMEM supplemented with 10% fetal bovine serum (Hyclone; SH30071.03), 1x glutamax, 1x penicillin/streptomycin, 1x sodium pyruvate, and 10 mM HEPES (Life Technologies) Genotyped Epstein Barr immortalized B cells (BLCLs) (Supplementary Table 1) were obtained from Coriell Institute and cultured as specified by vendor[26].

Plasmids and mRNA

Transient expression vectors encoding TASL, IRF5, and IRF7 into PCMV entry vector were purchased from Origene (#RC204618, # MR226592, #MR225814). Site-Directed Mutagenesis using the Quickchange II kit (Agilient; 200522) was used to create Rs887369 alleles. C-terminal HA tagged variants were generated via subcloning into the PCMV-AC-HA vector from Origene. For generation of mRNA, human TASL, human

https://doi.org/10.1038/s41467-024-55690-0

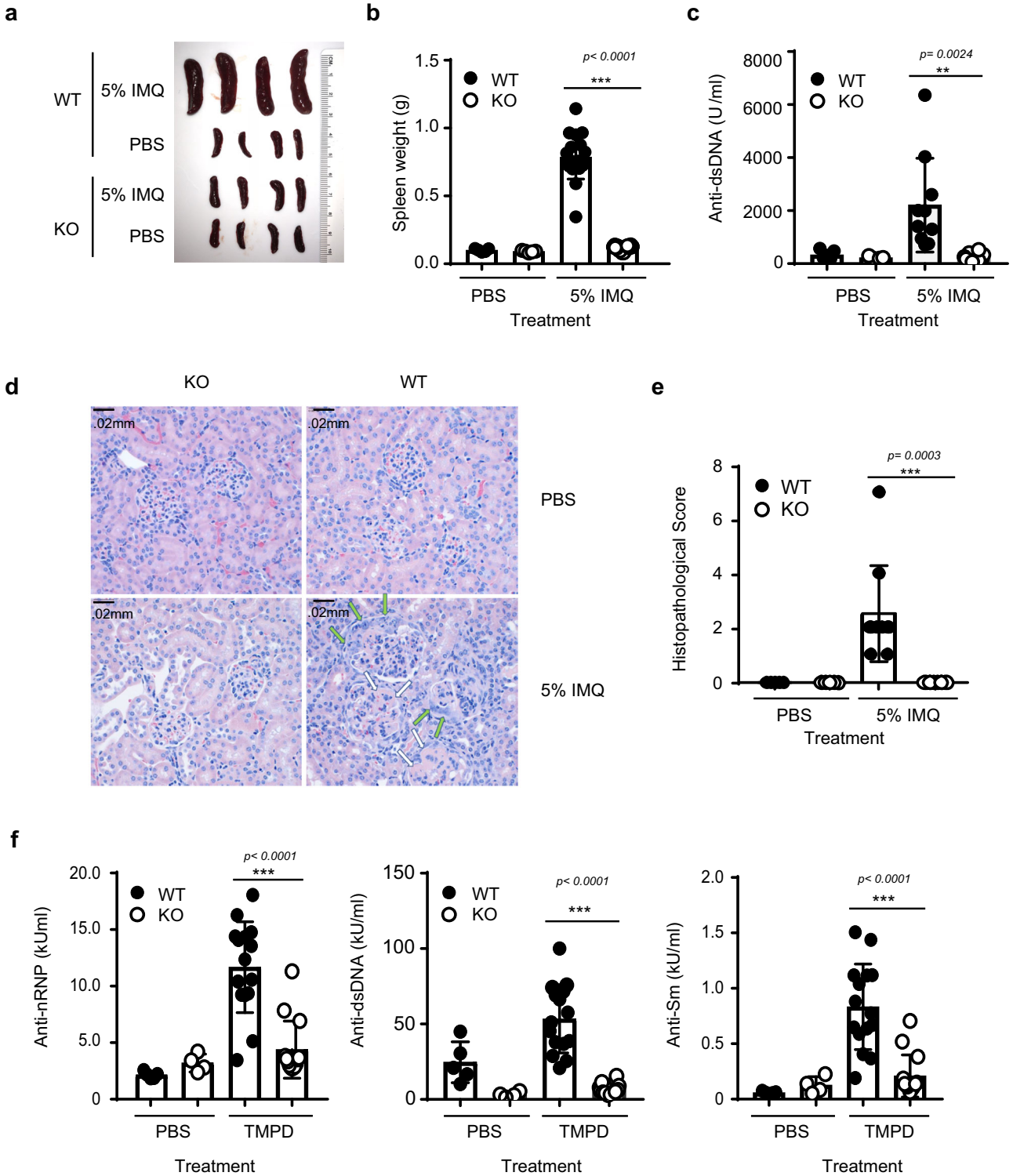

Fig. 3 | *Tasl*$^{-/-}$ mice are protected in mouse models of SLE. Wild type control littermates (WT) and *Tasl*$^{-/-}$ (KO) mice were treated with either (PBS) or 5% imiquimod (IMQ; Aldara) three times per week and analyzed after 8 weeks. **a** Representative macroscopic images of spleens. **b** Mouse spleen weights for treatment groups PBS ($n = 5$) and IMQ ($n = 20$). **c** Serum levels of anti-dsDNA antibodies. PBS ($n = 5$), IMQ ($n = 10$). **d** Representative microscopic images of H&E stained kidney sections. Affected glomeruli are characterized by enlargement and segmental sclerosis with increased hyalinized mesangial matrix (white arrows) and hypertrophy/ hyperplasia of epithelial cells lining Bowman's capsules (green arrows). **e** Renal histopathological scores in mice. PBS ($n = 5$), IMQ ($n = 10$). **f** Wild type control littermates (WT) and *TASL*$^{-/-}$ (KO) mice were injected with either (PBS) (WT $n = 5$, KO $n = 4$) or a single dose of TMPD (pristane) (WT $n = 15$, KO $n = 14$) and serum anti-nRNP, anti-dsDNA, and anti-Sm autoantibodies were measured 8 months post injection. In (**b**, **c**) and (**e**, **f**), data are means ± SEM and are representative of 2 independent experiments. Unpaired t test (2 tailed) *** $P < 0.0005$; ** $P < 0.005$. Images in (**a**) and (**d**) are representative of two independent experiments.

https://doi.org/10.1038/s41467-024-55690-0

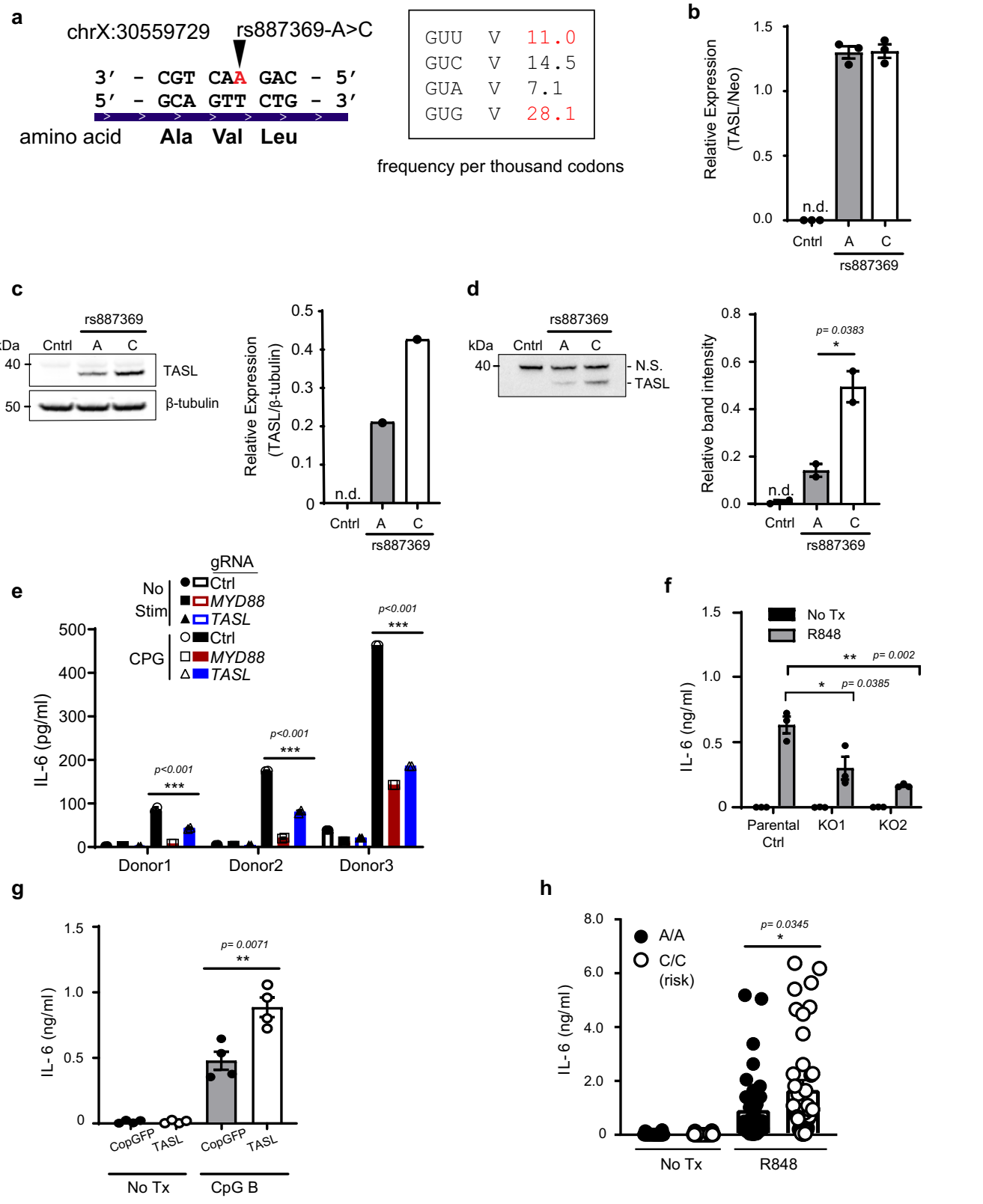

TASL-HA, CopGFP derived from pCDH-EF1α-MCS-(PGK-CopGFP) vector (System Biosciences; CD811A-1), and IRF7 fused to CopGFP were cloned into the pMRNAxp vector system (System Biosciences; MR-KIT-1) for use as an mRNA template vector. 5′ capped (CAP1) mRNA with N1-methylpseudouridine modifications encoding CopGFP, CopGFP-IRF7, human TASL, and Human TASL-HA was custom synthesized by TriLink Biotechnologies Inc using mRNA template vectors.

Mouse primary cell isolation and culture

Bone marrow cells were extracted from femurs from 6–10 week old female *Tasl*$^{-/-}$ (KO) and wild type (WT) littermates and cultured in 100 ng/ml Flt3L (R&D Systems; 427-FL-025) for 7–10 days to generate DCs according to standard techniques. B cells and pDCs were isolated from spleens of each genotype with B cell isolation kit and pDC isolation kit from Miltenyi Biotec (130-090-862, 130-107-093) according

Fig. 4 | SLE associated SNP affects TASL expression. a DNA and codon triplet sequence of rs887369 alleles for reference (A) and SLE risk variant (C) and codon usage table for Val tRNA frequencies. **b** HEK293T cells were transfected with either an empty vector (Ctrl) or FLAG tagged TASL expression vectors containing either the rs887369-A SNP or the rs887369-C SNP (risk variant). RT-qPCR analysis of TASL mRNA expression in transfected cells. TASL expression was normalized to neomycin(Neo) resistance cassette co-expressed in the vectors. **c** Western blot analysis using anti-FLAG (TASL) and β-tubulin (loading control) antibodies. Right panel is quantification of western blot. **d** Western blot analysis of TASL protein from an in vitro translation assay using FLAG tagged TASL expression vectors containing either the rs887369-A SNP, the rs887369-C SNP (risk variant), or an empty vector (ctrl). N.S. indicates a non-specific protein band. Right panel indicates quantification of TASL bands from two independent experiments normalized to non-specific protein band. **e** B cells were isolated from PBMCs ($n = 3$ donors) and were electroporated with Cas9 complexed with either control or gRNAs targeting *TASL* or *MYD88*. Cells were stimulated with CpG B and IL-6 was measured 24 h later by CBA. **f** BLCLs were transfected with Cas9 complexed with either control gRNAs (Parental Ctrl) or gRNAs targeting *TASL* (KO1, KO2). Cells were stimulated with R848 (10μg/ml) overnight and IL-6 was measured. **g** human B cells isolated from PBMCs were transfected with mRNA encoding either TASL or CopGFP and stimulated with CpG B. IL-6 was measured 24 h later by CBA. **h** BLCLs derived from carriers homozygous for either the A or C(risk) rs887369 allele were stimulated with R848 ($n = 42$). IL-6 was measured from the supernatant 24 h post stimulation. Data are means ± SEM and are representative of at least 2 independent experiments. In (**d**), (**f**), (**g**), and (**h**) Unpaired *t* test (2-tailed) $^{**}P < 0.01$, $^{*}P < 0.05$. **e** Two-way ANOVA $^{***}P < 0.001$.

to manufacturer's instructions. All cell lines were cultured in RPMI with above described supplements unless otherwise specified.

Cell treatments and analysis of cytokines

BLCLs were stimulated with R848 (10 μg/ml) for 24 h before supernatants were harvested. Splenic B cells were isolated from naïve mice with Miltenyi B cell isolation kit as described above and were stimulated for 48 h as outline with LPS (10μg/ml), R837 (10 μg/ml) or CpG A (ODN 2216 2μM), all from Invivogen (tlrl-b5lps, tlrl-imqs, tlrl-2216). Splenic pDCs and bone marrow Flt3L derived pDCs were stimulated with polyI:C (50 μg/ml;Millipore528906), LPS (5μg/ml), R848 (10μg/ml;tlrl-r848), CpG A (ODN 2216 3μM; tlrl-2216), CpG B (ODN 1668 3 μM or 10 μg/ml; tlrl-1668), ISD (4μg/ml; tlrl-isdn), 5'ppp dsRNA (2μg/ml; tlrl-3prna)—all from Invivogen. ISD and 5p'dsRNA were complexed with Lipofectamine 2000 (Thermo Fisher Scientific; 11668019) IL-6 and TNF from collected supernatants were assessed by Cytometric Bead Array Flex kits (BD Biosciences; 558301, 562336). Mouse IFN-α and IFN-β detection from supernatants was measured using Verikine mouse IFN-α and High sensitivity IFN-β ELISA kit (PBL; 42120, 42410). IFN-α from serum was measured by Verikine mouse high sensitivity IFN-α ELISA kit (PBL;42115). Plasmacytoid dendritic cells were stimulated with 500U/ml (PBL; 11200-2)

Western blots and antibodies

Cells were lysed in 1x RIPA buffer (SIGMA; 20-188) supplemented with 1% TritonX-100 and 1x Halt protease & phosphatase inhibitor (Invitrogen; 78440). The protein concentration in the lysates was determined by BCA protein assay kit (Thermo Fisher Scientific; 23250). The samples were boiled with NuPAGE LDS sample buffer (Invitrogen; 1920134) including reducing agent (Invitrogen; 1879834). Sample were ran on Bolt 4–12% Bis-Tris gels (Invitrogen) in MES SDS running buffer then transferred onto nitrocellulose membrane (Invitrogen; IB23002) using iBlot2 system (Invitrogen). Western blots were stained, visualized, and quantified using the Licor Odyssey Imager system per manufacturer's instructions. The following antibodies were purchased from Invitrogen: AlexaFluor 800 plus anti-Rabbit IgG (A32735), AlexaFluor 800 plus anti-mouse IgG (A32730), AlexaFluor 680 plus anti-mouse IgG (A32729), AlexaFluor 680 plus anti-rabbit IgG (A32734), anti-TLR7 N terminus (PA112829), anti-CopGFP(PA5-22688), anti-p-IRF5(PA5-64760). The following antibodies were purchased from Abcam: rabbit anti-IRF5 (ab181553). The following antibodies were purchased from Cell signaling technology: anti-IRF7 (4920), anti-Flag tag (14793), anti-HA-tag (3724), anti-beta-actin (3700), anti-tubulin (86298), anti-GAPDH (2118), anti-Histone H3 (9715), p-STAT1 (9167), STAT1 (9172), p-IkBa (2859), IkBa (4812), p38 (8690), p-p38 (4511). Anti-mouse TLR9 TIR domain serum, anti-mouse TLR9 antibody (J15A7), and anti- mouse TLR7 antibody (A94B10) was a gift from K. Miyake (University of Tokyo)[14,16]. AlexaFluor secondary detection antibodies were used at dilution of 1:5000. Anti-beta-actin, anti-tubulin, anti-GAPDH, anti-Histone H3 antibodies were used at a dilution of 1:3000. Anti-pIRF5, p-IkBa, p-p38, and p-STAT1 were used a dilution of 1:500. All other antibodies were used at a dilution of 1:1000.

Nuclear and cytosolic fractionation

Fractionation of cytosol and nuclear fractions in Flt3L derived pDCs from 6–10 week old female *Tasl*$^{-/-}$ (KO) and wild type (WT) littermates was achieved using the CelLytic NuCLEAR Extraction Kit (Sigma Aldrich; NXTRACT-1KT) with the following modifications. For each time point, 20million pDC cells were used for fractionation. 1x Halt protease and phosphatase inhibitor was added to each buffer extraction step. Harvested pDC cell pellets were resuspended in 750ul of isotonic lysis buffer and cytosolic fractions were harvested according to manufacturer's instructions with a final concentration of 0.3% IGEPAL CA-630 (Sigma Aldrich; I8896). Nuclear fractions were collected per manufacturer's instructions after incubation of nuclei with extraction buffer for 30 min shaking at 1200RPMs.

In vitro translation assay and quantification of TASL

In vitro translation assay was performed using the 1-Step Human coupled IVT kit (ThermoFisher Scientific; 88881). Human *TASL* containing either the rs887369-A or rs887369-C SNP was cloned into pCDNA3.1 plasmid (Invitrogen; V79020) and used as a template for the IVT reaction. HEK293T were transfected (Lipofectamine 2000) with constructs expressing TASL SNPs and lysed in RIPA buffer (EMD Millipore).

Immunoprecipitation experiments

For immunoprecipation of TLRs, 15 ug of either anti- mouse TLR7 antibody (A94B10) or 15 μg of anti-mouse TLR9 antibody (J15A7) were conjugated to 75 μl of protein G magnetic Dynabeads (ThermoFisher; 10003D) per manufacturer's instructions. 6 million HEK293T cells stably expressing indicated TLRs or 30 million pDCs per genotype were lysed in lysis buffer (1% Lubrol, 20 mM Tris/HCl (pH 7.4), 150 mM NaCl, 1 mM CaCl2, 1 mM MgCl2, 10% glycerol, 1x Halt protease and phosphatase inhibitor (Thermo Scientific; 78440) and clarified lysate was incubated with antibody conjugated protein G beads overnight at 4 °C. Beads were washed 3 times in wash buffer (0.2% Lubrol, 20 mM Tris/HCl (pH 7.4), 150 mM NaCl, 1 mM CaCl2, 1 mM MgCl2, 10% glycerol) and eluted in 1x LDS loading buffer (Invitrogen; 1920134) plus 1x reducing reagent (Invitrogen; 1879834) at 70 °C for 10–20 min. Input and eluted samples were ran on a 4–12% Bolt Bis-Tris Gel (Invitrogen; NW04120BOX) and transferred to a PVDF membrane (Invitrogen; IB24001) using the iBlot2 system (Invitrogen) for western blot analysis. Anti-mouse TLR9 TIR domain serum[14,16] and anti-TLR7 N terminus (Invitrogen;PA112829) were used to detect TLR9 and TLR7 respectively.

CRISPR deletion in BLCLs

Guide RNA oligos (Alt-R crRNA XT) were purchased from IDT and complexed with tracerRNA to form gRNA duplexes according to manufacturer's instructions. Recombinant TrueCut ver2

Cas9(Invitrogen; A36498) was purchased from. 1 million BLCL cell from donor HG01784 were resuspended in SF nucleofector buffer (Lonza Biosciences;V4XC-1032) and incubated with Cas9-RNP complex consisting of 180pmol of Cas9 and 160pmol of gRNA duplexes. Cells were electroporated using the Amaxa 4-D nucleofector system (Lonza Bioscience), program DN-100. Two guide RNAs were used for generation of each KO and parental control cell line. KO1: gRNA1: tccagcggtactcatcctat, gRNA2: gtagaaatggaatcctccat. KO2: gRNA1: agtactggaatgacatccac, gRNA2: atctcagtggacttgagtac. Parental control: IDT negative control gRNA #1 (IDT; 1072544) and negative control gRNA #2 (IDT; 1072545). Generation of KOs and validation of gRNAs was confirmed using the Surveyor mutagenesis assay kit (IDT) according to manufacturer's instructions (IDT; 706025). *TASL* was PCR amplified from genomic DNA isolated from BLCL lines and used as the surveyor assay template.

Primary human B cell isolation, CRISPR, and mRNA transfection

Human PBMCs from healthy volunteers were obtained through informed consent via the Amgen Research Blood Donor Program. Culturing and genetic manipulation of primary human B cells was performed[40]. Human B cells were isolated from freshly purified PBMCs using the EasyStep B cell isolation kit (Stem Cell Technologies; 17954) per manufacturer's instructions. B cells were first cultured and expanded in B cell media StemMACS HSC Expansion Media XF (Miltenyi; 130-100-463) containing 1x Pen/Strep (Invitrogen), 5% human AB serum (Sigma;H3667), 125 IU/mL of human IL-4 (Miltenyi; 130-093-922), and 8 U/ml of multimeric CD40 ligand (Miltenyi; 130-098-775). Media was changed every 3–4 days. For CRISPR deletion, day 7–9 cultured B cells were electroporated with 180pmol of Cas9 and 160pmol gRNA:tracer using the Amaxa primary buffer-2, 4-D nucleofector kit (Lonza Biosciences; V4XP-2032) using program CM137. The following two gRNAs pairs were purchased from IDT and used to generate the indicated CRISPR KO groups: Ctrl (IDT ctrl gRNA#1, negative control gRNA#2), Myd88 (gttcttgaacgtgcggacac, gtacttggagatccggcaac), and TASL (agtactggaatgacatccac, gtagaaatggaatcctccat). After electroporation, cells were cultured in B cell media without CD40 ligand for 3 days, and then transferred to fresh B cell media without CD40 ligand & IL-4, and stimulated with 3uM CpG B ODN2006 for 24 h. For mRNA transfection, day 4 cultured cells were electroporated with 300 ng of either CopGFP or TASL mRNA via the Amaxa primary buffer-2, 4-D nucleofector kit using buffer p2 and program CM137 (Lonza biosciences; V4XP-2032). After mRNA electroporation, cells were cultured in fresh B cell media without CD40 ligand for two days, and then stimulated with 3uM of CpG B ODN2006 for 24 h.

CopGFP-IRF7 microscopy

3.5 million bone marrow Flt3L derived pDCs were electroporated with 1 µg of CopGFP-IRF7 mRNA using program CM137, buffer P2 with the 4-D nucleofector system (Lonza biosciences; V4XP-2032). After electroporation, cells were seeded onto a 12 mm pre-coated collagen glass coverslips(Neuvitro; G-12-collagen) in a 24-well dish containing 1 ml of pDC media. Media was changed every day. Three days post-electroporation, cells were then stimulated with 3uM of CpG A (Invivogen; tlrl-2216) for 6 h. After stimulation, cells were wash 3 times in PBS and fixed with 2% paraformaldehyde. Coverslips were mounted onto glass slides with ProLong Diamond antifade mount with DAPI (ThermoFisher; P36962). Cells were visualized using a Leica SP8 laser scanning confocal microscope. 100 cells per coverslip were analyzed for the percent colocalization of CopGFP with DAPI and the average of three coverslips per group was plotted.

Serologic analysis of autoantibodies

Anti-double-stranded DNA (anti-dsDNA IgG-specfic), anti-nRNP (Ig total A + G + M), and anti-Sm antibodies were measured via ELISA kits (Alpha Diagnostic; 5120, 5410) according to manufacturer's instructions.

FACS analysis

The following antibodies at the indicated dilutions were used - BD Biosciences: CD8 BUV395 (1:200, clone 53-6.7), CD4 BUV496 (1:400, GK1.5), and Ly6G BUV395 (1:400, 1A8), CD21/CD35 PE (1:400, 7G6), mouse TLR7 PE (1:100, A94B10), mouse TLR9 (1:100, J15A7). BioLegend: CD3 BV605 (1:200, 17A2), CD19 BV711 (1:200, 6D5), Ly6C (1:200, HK1.4), B220 BV711 (1:200, RA3-6B2), CD45 BV785(1:400, 30-F11), CD11c FITC or BV421 (1:200, N418), CD11b APC-Cy7 (1:200, M1/70), and I-A/I-E PECy7 (1:400, M5/114.15.2), CD23 APC (1:200, B3B4). eBioscience: CD317/PDCA-1 FITC (1:200, eBio927), Siglec-H PE (1:400, eBio440c), and F4/80 APC (1:400, BM8). Before staining for surface markers, cells were incubated with an anti CD16/32 antibody (1:400, 2.4G2, BD Biosciences) and dead cells were excluded using a fixable live/dead stain (1:1000, eBioscience; 65-2860-40) or 7AAD(1:2000, Biologend; 420403). All stains were carried out in PBS containing 3% FBS (v/v) or Brilliant stain buffer (BD Biosciences). Cells were stained for at least 20 min at 4 °C with antibodies. Doublets (FSC-H vs FSC-A) and dead cells were excluded, and all cell populations were gated on $CD45^+$. T cells were isolated as $CD4^+$ or $CD8^+$ within $CD19^-$ $CD3^+$ subpopulation. B cells were isolated as $CD19^+$. Marginal zone B cells were isolated as $CD23^{lo/-}CD21^{hi}$ and follicular B cells were isolated as $CD23^{hi}CD21^{int}$ within $B220^+$ population. Myeloid populations were all gated on $CD3^-$. Neutrophils were isolated as $CD11b^+$ $Ly6G^+$. Monocytes as $CD11b^+$ $Ly6C^+$ $Ly6G^-$. cDCs as $CD11c^+$ I-A/I-$E^+$$Ly6C^-$ $Ly6G^-$. Macrophages as $F4/80^+$ I-A/I-E^+ $Ly6C^-$ $Ly6G^-$. pDCs as $SiglecH^+$ $B220^+$ within $CD11c^+$ I-A/I-E^+ cDC subpopulation. Data were collected on LSR II or Symphony (BD Biosciences) and analyzed on FlowJo software.

Quantitative PCR

Total RNA was isolated with RNA Clean & Concentrator kit (Zymo; R1017) and reverse transcribed using SuperScript IV VILO Master mix (Invitrogen; 11756050). For expression of *TASL* from human tissues or TLR7/9 expression from splenocytes of *Tasl*$^{-/-}$ and littermate control, female 6–8 weeks of age, cDNA was used with TaqMan Gene Expression Master Mix from Applied Biosystems. The following TaqMan Gene Expression Assay probes were purchased from Invitrogen (Human *TASL*: Hs00958259_m1, Human *GAPDH*: Hs02786624, Mouse *Tlr7*: Mm00446590_m1, Mouse *Tlr9*: Mm00446193_m1). Gene-specific transcript levels were normalized to mRNA of *GAPDH*. For RT-qPCR of mouse *Tasl*(*5430427O19Rik)* cell type expression, the SYBR Green Universal Master mix (Applied Biosystems) assay was with the following primer pairs: *TASL*-Forward 5′- TATAATGAACCGGTGGCTGGG -3′, Reverse 5′ AGAAGCCAGAGCAGAACAGT 3′ and normalized to *HPRT:* Forward 5′- GGCCAGACTTTGTTGGATTT-3′, Reverse 5′- ATGAGCGCAAGTTGAATCTG -3′For IVT assay mouse SYBR primers for TASL (see above) were used and normalized to *Neo:* Forward 5′ CAAGATGGATTGCACGCAGG 3′, Reverse 5′TTCAGTGACAACGTCGAGCA 3′ Samples were run on Viia7 Real-Time PCR System (Thermo Fisher).

Reporting summary

Further information on research design is available in the Nature Portfolio Reporting Summary linked to this article.

Data availability

All data are included in the Supplementary Information or available from the authors, as are unique reagents used in this Article. The raw numbers for charts and graphs are available in the Source Data file whenever possible. Source data are provided with this paper.

References

1. Weckerle, C. E. & Niewold, T. B. The unexplained female predominance of systemic lupus erythematosus: Clues from genetic and cytokine studies. *Clin. Rev. Allergy Immunol.* **40**, 42–49 (2011).
2. Kirou, K. A. & Gkrouzman, E. Anti-interferon alpha treatment in SLE. *Clin. Immunol.* **148**, 303–312 (2013).

3. Isenberg, D. A. B cell targeted therapies in autoimmune diseases. *J. Rheumatol. Suppl.* **77**, 24–28 (2006).
4. Baechler, E. C. et al. Interferon-inducible gene expression signature in peripheral blood cells of patients with severe lupus. *Proc. Natl. Acad. Sci. USA* **100**, 2610–2615 (2003).
5. Rowland, S. L. et al. Early, transient depletion of plasmacytoid dendritic cells ameliorates autoimmunity in a lupus model. *J. Exp. Med.* **211**, 1977–1991 (2014).
6. Davison, L. M. & Jorgensen, T. N. Sialic acid-binding immunoglobulin-type lectin H-positive plasmacytoid dendritic cells drive spontaneous lupus-like disease development in B6.Nba2 mice. *Arthritis Rheumatol.* **67**, 1012–1022 (2015).
7. Boule, M. W. et al. Toll-like receptor 9-dependent and -independent dendritic cell activation by chromatin-immunoglobulin G complexes. *J. Exp. Med.* **199**, 1631–1640 (2004).
8. Leadbetter, E. A. et al. Chromatin-IgG complexes activate B cells by dual engagement of IgM and Toll-like receptors. *Nature* **416**, 603–607 (2002).
9. Deane, J. A. et al. Control of toll-like receptor 7 expression is essential to restrict autoimmunity and dendritic cell proliferation. *Immunity* **27**, 801–810 (2007).
10. Majer, O., Liu, B., Kreuk, L. S. M., Krogan, N. & Barton, G. M. UNC93B1 recruits syntenin-1 to dampen TLR7 signalling and prevent autoimmunity. *Nature* **575**, 366–370 (2019).
11. Bentham, J. et al. Genetic association analyses implicate aberrant regulation of innate and adaptive immunity genes in the pathogenesis of systemic lupus erythematosus. *Nat. Genet* **47**, 1457–1464 (2015).
12. Langefeld, C. D. et al. Transancestral mapping and genetic load in systemic lupus erythematosus. *Nat. Commun.* **8**, 16021 (2017).
13. Heinz, L. X. et al. TASL is the SLC15A4-associated adaptor for IRF5 activation by TLR7-9. *Nature* **581**, 316–322 (2020).
14. Fukui, R. et al. Cleavage of toll-like receptor 9 ectodomain is required for in vivo responses to single strand DNA. *Front Immunol.* **9**, 1491 (2018).
15. Pelka, K. et al. The Chaperone UNC93B1 regulates toll-like receptor stability independently of endosomal TLR transport. *Immunity* **48**, 911–922 e917 (2018).
16. Onji, M. et al. An essential role for the N-terminal fragment of toll-like receptor 9 in DNA sensing. *Nat. Commun.* **4**, 1949 (2013).
17. Kanno, A. et al. Targeting cell surface TLR7 for therapeutic intervention in autoimmune diseases. *Nat. Commun.* **6**, 6119 (2015).
18. Kawasaki, T. & Kawai, T. Toll-like receptor signaling pathways. *Front Immunol.* **5**, 461 (2014).
19. Takaoka, A. et al. Integral role of IRF-5 in the gene induction programme activated by toll-like receptors. *Nature* **434**, 243–249 (2005).
20. Pandey, A. K. et al. NOD2, RIP2 and IRF5 play a critical role in the type I interferon response to Mycobacterium tuberculosis. *PLoS Pathog.* **5**, e1000500 (2009).
21. Yokogawa, M. et al. Epicutaneous application of toll-like receptor 7 agonists leads to systemic autoimmunity in wild-type mice: a new model of systemic Lupus erythematosus. *Arthritis Rheumatol.* **66**, 694–706 (2014).
22. Reeves, W. H., Lee, P. Y., Weinstein, J. S., Satoh, M. & Lu, L. Induction of autoimmunity by pristane and other naturally occurring hydrocarbons. *Trends Immunol.* **30**, 455–464 (2009).
23. Newman, Z. R., Young, J. M., Ingolia, N. T. & Barton, G. M. Differences in codon bias and GC content contribute to the balanced expression of TLR7 and TLR9. *Proc. Natl Acad. Sci. USA* **113**, E1362–E1371 (2016).
24. Hunt, R. C., Simhadri, V. L., Iandoli, M., Sauna, Z. E. & Kimchi-Sarfaty, C. Exposing synonymous mutations. *Trends Genet* **30**, 308–321 (2014).
25. Athey, J. et al. A new and updated resource for codon usage tables. *BMC Bioinforma.* **18**, 391 (2017).
26. International HapMap, C. et al. Integrating common and rare genetic variation in diverse human populations. *Nature* **467**, 52–58, (2010).
27. Cao, W. et al. Toll-like receptor-mediated induction of type I interferon in plasmacytoid dendritic cells requires the rapamycin-sensitive PI(3)K-mTOR-p70S6K pathway. *Nat. Immunol.* **9**, 1157–1164 (2008).
28. Hua, Z. & Hou, B. TLR signaling in B-cell development and activation. *Cell Mol. Immunol.* **10**, 103–106 (2013).
29. Arazi, A. et al. The immune cell landscape in kidneys of patients with lupus nephritis. *Nat. Immunol.* **20**, 902–914 (2019).
30. Purtha, W. E., Swiecki, M., Colonna, M., Diamond, M. S. & Bhattacharya, D. Spontaneous mutation of the Dock2 gene in Irf5-/- mice complicates interpretation of type I interferon production and antibody responses. *Proc. Natl. Acad. Sci. USA* **109**, E898–E904 (2012).
31. Yasuda, K. et al. Phenotype and function of B cells and dendritic cells from interferon regulatory factor 5-deficient mice with and without a mutation in DOCK2. *Int Immunol.* **25**, 295–306 (2013).
32. Yasuda, K. et al. Interferon regulatory factor-5 deficiency ameliorates disease severity in the MRL/lpr mouse model of lupus in the absence of a mutation in DOCK2. *PloS One* **9**, e103478 (2014).
33. Blasius, A. L. et al. Slc15a4, AP-3, and Hermansky-Pudlak syndrome proteins are required for toll-like receptor signaling in plasmacytoid dendritic cells. *Proc. Natl Acad. Sci. USA* **107**, 19973–19978 (2010).
34. Consortium, G. T. et al. Genetic effects on gene expression across human tissues. *Nature* **550**, 204–213 (2017).
35. Berletch, J. B. et al. Escape from X inactivation varies in mouse tissues. *PloS Genet* **11**, e1005079 (2015).
36. Souyris, M. et al. TLR7 escapes X chromosome inactivation in immune cells. *Sci. Immunol* **3**, https://doi.org/10.1126/sciimmunol.aap8855 (2018).
37. Lambert, N. C. Nonendocrine mechanisms of sex bias in rheumatic diseases. *Nat. Rev. Rheumatol.* **15**, 673–686 (2019).
38. Dillon, S. et al. Klinefelter's syndrome (47,XXY) among men with systemic lupus erythematosus. *Acta Paediatr.* **100**, 819–823 (2011).
39. Bajema, I. M. et al. Revision of the International Society of Nephrology/Renal Pathology Society classification for lupus nephritis: Clarification of definitions, and modified National Institutes of Health activity and chronicity indices. *Kidney Int* **93**, 789–796 (2018).
40. Johnson, M. J., Laoharawee, K., Lahr, W. S., Webber, B. R. & Moriarity, B. S. Engineering of primary human B cells with CRISPR/Cas9 targeted nuclease. *Sci. Rep.* **8**, 12144 (2018).

Acknowledgements

We would like to thank the University of Tokyo and Dr. Kensuke Miyake for providing Toll-like receptor antibody reagents and protocols.

Author contributions

L.L, A.S.R, and T.A.C. performed and analyzed in-vivo studies. J.L. scored and analyzed all histology studies. L.L, W.E.P, A.S.R, and R.H performed and analyzed all flow cytometry studies. L.L, A.C., H.K., performed and analyzed in vitro cell line and primary cell studies. D.N.B. and M.J.R. analyzed and interpreted data. P.S.M, B.W.G., W.O., and J.D. supervised studies. P.S.M designed studies and wrote manuscript with input from all authors.

Competing interests

All authors were employees of Amgen Inc. at time of studies. L.L, T.A.C, W.O, and P.S.M are current employees of Gilead Inc. R.H. is a current employee of Genentech Inc. A.C. is a current employee of Exelixis. D.N.B., M.J.R., J.H.L., and J.D. are current employees of Amgen Inc.

Additional information

Supplementary information The online version contains supplementary material available at https://doi.org/10.1038/s41467-024-55690-0.

Correspondence and requests for materials should be addressed to Paolo S. Manzanillo.

Peer review information *Nature Communications* thanks Marta Alarcón-Riquelme and the other anonymous reviewer(s) for their contribution to the peer review of this work.